Am J Physiol Gastrointest Liver Physiol 305: G900–G910, 2013.
First published October 17, 2013; doi:10.1152/ajpgi.00265.2013.

Gut-derived short-chain fatty acids are vividly assimilated into host carbohydrates and lipids

Gijs den Besten,[1,4] Katja Lange,[3,4] Rick Havinga,[1] Theo H. van Dijk,[2] Albert Gerding,[2] Karen van Eunen,[1,4] Michael Müller,[3,4] Albert K. Groen,[1,2,4] Guido J. Hooiveld,[3,4] Barbara M. Bakker,[1,4] and Dirk-Jan Reijngoud[1,2,4]

[1]*Department of Pediatrics, Center for Liver, Digestive, and Metabolic Diseases, University of Groningen, University Medical Center Groningen, Groningen, The Netherlands;* [2]*Department of Laboratory Medicine, University of Groningen, University Medical Center Groningen, Groningen, The Netherlands;* [3]*Nutrition, Metabolism and Genomics Group, Wageningen University, Wageningen, The Netherlands; and* [4]*Netherlands Consortium for Systems Biology, Amsterdam, The Netherlands*

Submitted 13 August 2013; accepted in final form 10 October 2013

den Besten G, Lange K, Havinga R, van Dijk TH, Gerding A, van Eunen K, Müller M, Groen AK, Hooiveld GJ, Bakker BM, Reijngoud DJ. Gut-derived short-chain fatty acids are vividly assimilated into host carbohydrates and lipids. *Am J Physiol Gastrointest Liver Physiol* 305: G900–G910, 2013. First published October 17, 2013; doi:10.1152/ajpgi.00265.2013.—Acetate, propionate, and butyrate are the main short-chain fatty acids (SCFAs) that arise from the fermentation of fibers by the colonic microbiota. While many studies focus on the regulatory role of SCFAs, their quantitative role as a catabolic or anabolic substrate for the host has received relatively little attention. To investigate this aspect, we infused conscious mice with physiological quantities of stable isotopes [1-^{13}C]acetate, [2-^{13}C]propionate, or [2,4-$^{13}C_2$]butyrate directly in the cecum, which is the natural production site in mice, and analyzed their interconversion by the microbiota as well as their metabolism by the host. Cecal interconversion, pointing to microbial cross-feeding, was high between acetate and butyrate, low between butyrate and propionate, and almost absent between acetate and propionate. As much as 62% of infused propionate was used in whole body glucose production, in line with its role as gluconeogenic substrate. Conversely, glucose synthesis from propionate accounted for 69% of total glucose production. The synthesis of palmitate and cholesterol in the liver was high from cecal acetate (2.8 and 0.7%, respectively) and butyrate (2.7 and 0.9%, respectively) as substrates, but low or absent from propionate (0.6 and 0.0%, respectively). Label incorporation due to chain elongation of stearate was approximately eightfold higher than de novo synthesis of stearate. Microarray data suggested that SCFAs exert a mild regulatory effect on the expression of genes involved in hepatic metabolic pathways during the 6-h infusion period. Altogether, gut-derived acetate, propionate, and butyrate play important roles as substrates for glucose, cholesterol, and lipid metabolism.

gut-microbial metabolism; lipid metabolism; glucose metabolism; metabolic regulation

SHORT-CHAIN FATTY ACIDS (SCFAs), of which acetate, propionate, and butyrate are the most abundant, are the main products of fermentation of dietary fibers by the anaerobic colonic microbiota (11). In the last decades it became apparent that SCFAs might play a key role in the prevention and treatment of metabolic syndrome, bowel disorders, and certain types of cancer (14, 17, 45, 47). In clinical studies SCFA administration reduced symptoms related to ulcerative colitis, Crohn's disease, and antibiotic-associated diarrhea (4, 6, 13, 18, 51).

SCFAs are substrates for energy metabolism in the host (11). The average human diet in Western societies yields 300–600 mmol SCFAs/day, which is equivalent to ~10% of the human caloric daily requirements (3). In the passage from the lumen of the gut to the hepatic vein SCFAs are actively metabolized by colonocytes in the order of butyrate > acetate > propionate (41). The remainder of the SCFAs is largely taken up by the liver (5). Quantitative insight into the partitioning of SCFAs over the subsequent metabolic routes is lacking. According to known biochemical pathways, acetate can be oxidized in the tricarboxylic acid (TCA) cycle or can be used as a substrate for synthesis of cholesterol, ketone bodies, and long-chain fatty acids. Butyrate is supposed to enter mitochondrial fatty acid oxidation and the resulting acetyl-CoA can be used in similar ways as acetate. This leads to the hypothesis that label incorporation from butyrate will resemble that from acetate. Propionate is a well-known precursor for gluconeogenesis in the liver (42), but whether it is used for lipogenesis has not been studied. Detailed analysis of SCFA as substrates was mostly performed in vitro in isolated cell lines derived from colonocytes or hepatocytes, which gives only a limited view on the processes in vivo (2, 7, 10, 33, 41).

The interpretation of available in vivo SCFA studies is complicated by the different administration routes of SCFAs to the host. While the natural production of SCFAs occurs mainly in the cecum, in experiments they are usually administered via food, via intraperitoneal injection, or via intravenous infusion (17, 21, 27, 36). This is likely to affect their impact on energy metabolism via the hormonal and regulatory responses that are triggered in different organs (19, 26).

In this study we present a new mouse model in which we infused conscious mice with stable isotope-labeled SCFAs directly in the cecum at a delivery rate of 2.4 mmol·kg body $wt^{-1}\cdot h^{-1}$. This infusion rate was estimated to be on the higher side of the physiological range, high enough to ensure substantial isotope enrichment in metabolic end products of SCFAs. To our knowledge, there are no accurate in vivo SCFA production rates published in mice, but there are data from in vitro and in vivo studies in other species. In 12-h-fasted humans the in vivo acetate production was estimated to be 0.75 mmol·kg body $wt^{-1}\cdot h^{-1}$, whereas it was 1.46 and 1.75 mmol·kg body $wt^{-1}\cdot h^{-1}$ in 24-h-fasted dogs and 22-h-fasted rats, respectively (36). The total SCFA production was 2.02 mmol·kg body $wt^{-1}\cdot h^{-1}$ in 22-h-fasted rats (36). It is expected that rates will

Address for reprint requests and other correspondence: D.-J. Reijngoud, Hanzeplein 1, 9713 GZ Groningen, The Netherlands (e-mail: D.J.Reijngoud01@umcg.nl).

substantially increase particularly in animals fed a fiber-rich diet. By infusing labeled SCFAs at their natural production site at a physiological rate, we get insight into the contributions of biochemical pathways used by the different SCFAs. The results reveal *1*) extensive in vivo microbial conversion of SCFAs, compatible with cross-feeding, *2*) vivid assimilation of gut-derived SCFAs in host carbohydrates and lipid, and *3*) conspicuous differences between the metabolism of the three SCFAs.

MATERIALS AND METHODS

Animals and experimental design. Male C57Bl/6J mice (Charles River, L'Arbresle Cedex, France), 2 mo of age, were housed in a light- and temperature-controlled facility (lights on 6:30 A.M. to 6:30 P.M., 21°C). Mice were fed a semisynthetic diet [based on D12450B (9); Research Diet Services, Wijk Bij Duurstede, The Netherlands] for 6 wk and had free access to drinking water. Experimental procedures were approved by the Ethics Committees for Animal Experiments of the University of Groningen.

Cecal infusion experiment. Mice were equipped with a permanent cecum catheter attached to the skull by acrylic glue under isoflurane anesthesia. Following the surgery, mice were allowed a recovery period of 5 days. Cecal cannulas were flushed daily with phosphate-buffered saline. On the day of the experiment, mice were individually housed and fasted from 6:00 to 10:00 A.M. All infusion experiments were performed in conscious, unrestrained mice. Four different groups received either a control phosphate-buffered saline solution, a 0.3 M sodium [1-^{13}C]acetate (99 atom%; Sigma-Aldrich) solution, a 0.3 M sodium [2-^{13}C]propionate (99 atom%; Sigma-Aldrich) solution, or a 0.3 M sodium [2,4-$^{13}C_2$]butyrate (99 atom%; Sigma-Aldrich) solution at pH 5.8 infused via the cecum catheter at an infusion rate of 0.2 ml/h. The resulting rate of infusion of labeled SCFA was 2.4 mmol·kg^{-1}·h^{-1}. The infusion rates needed to be high enough to ensure substantial isotope enrichment in metabolic end products of SCFAs. As a consequence, they turned out to be on the higher side of the physiological range. Every hour a blood sample was taken via tail bleeding on filter paper to determine the enrichment in glucose, cholesterol, and acylcarnitines. After 6 h of infusion, animals were killed by cardiac puncture under isoflurane anesthesia. Cecum content and livers were quickly removed, freeze-clamped, and stored at −80°C for fatty acid enrichment determination. Blood was centrifuged (4,000 *g* for 10 min at 4°C), and plasma was stored at −20°C to determine the enrichment in organic acids and amino acids.

Determination of enrichment and in vivo fluxes. Analytical procedures for extraction of glucose from blood spots, derivatization of the extracted compounds, and GC-MS measurements of derivatives were performed according to van Dijk et al. (50). In brief, glucose was extracted from blood spots using ethanol and converted to its pentaacetate derivative using pyridine/acetic anhydride (1:2 vol/vol) for 30 min at 60°C. Total cholesterol was extracted from blood spots using ethanol/acetone (1:1 vol/vol). Unesterified cholesterol from blood spots was subsequently derivatized using *N*,*O*-bis-(trimethyl)trifluoroacetamide with 1% trimethylchlorosilane at room temperature.

Enrichments of SCFAs and plasma organic acids were measured according to Moreau et al. (31) with minor modifications. In short, 100 μl of supernatant were spiked with 100 μl of internal standard (17.3 mM hydroxyisocapronic acid) and 20 μl of 20% 5-sulfosalicyclic acid. After a 10-min centrifugation the supernatant was acidified with 10 μl 37% HCl, and SCFA were extracted with 2 ml diethylether. Derivatization was performed overnight with 500 μl supernatant and 50 μl of *N-tert*-butyldimethylsilyl-*N*-methyltrifluoroacetamide. Enrichment of plasma amino acids was determined according to Hušek (22). In brief, plasma was denatured with acetonitrile, and amino acids were derivatized to *N*-ethoxycarbonyl ethyl esters using ethyl chloroformate at room temperature.

Liver homogenates were prepared in ice-cold phosphate-buffered saline, and different lipid fractions were obtained using thin-layer chromatography as described previously (49). Fatty acids were hydrolyzed in HCl-acetonitrile (1:22 vol/vol) for 45 min at 100°C. Fatty acids were extracted in hexane and derivatized for 15 min at room temperature using Br-2,3,4,5,6-pentafluorobenzyl/acetonitrile/triethanolamine (1:6:2 vol/vol). Derivatization was stopped by adding HCl, and the fatty acid-pentafluorobenzyl derivatives were extracted in hexane.

Mass isotopolog distributions were measured using an Agilent 5975 series GC/MSD (Agilent Technologies). Gas chromatography was performed using a ZB-1 column (Phenomenex). Mass spectrometry analysis was performed by electron capture negative ionization using methane as the moderating gas.

The normalized mass isotopolog distributions measured by GC-MS were corrected for natural abundance of ^{13}C by multiple linear regression according to Lee et al. (28) to obtain the excess fractional distribution of mass isotopologs. This distribution was used in mass isotopomer distribution analysis (MIDA) algorithms to calculate acetyl-CoA precursor pool enrichment, fractional palmitate synthesis rates, and the fraction of palmitate and oleate generated by elongation of de novo synthesized palmitate or by elongation of preexisting palmitate as described by Oosterveer et al. (35). The precursor pool enrichment is defined as the enrichment of the biosynthetic precursor subunits for newly synthesized polymers and the fractional synthesis as the fraction of polymer molecules in a mixture that were newly synthesized during the isotopic experiment (20).

Microarray analysis. High-quality total RNA was isolated using TRIzol reagent (Invitrogen) followed by DNase treatment and RNA column purification using the RNAeasy Mini Kit (Qiagen). Quality of all RNA samples was assessed with 6,000 Nano Chips using a bioanalyzer (Agilent Technologies) according to the manufacturer's instructions. Samples that showed an RNA integrity number above 8.0 were considered of suitable quality for pooled array hybridization. To this end, 3-μg RNA samples of each of the four to six mice per experimental group were pooled. Pooled total RNA (100 ng) was used for whole transcript cDNA synthesis using the Ambion WT expression kit (4411974; Applied Biosystems/Life Technologies), and subsequently labeled using the Affymetrix GeneChip WT Terminal Labeling Kit (901524; Affymetrix). Labeled RNA samples (5.5 μg) were hybridized on Mouse Gene 1.1 ST arrays (Affymetrix) and scanned in an Affymetrix GeneTitan instrument. Various advanced quality metrics, diagnostic plots, pseudoimages, and classification methods were used to determine the quality of the arrays before analysis (30). Probes were redefined using current genome information (8). In this study probes were reorganized based on the gene definitions as available in the Entez Gene database, version 38.1. Normalized expression estimates were obtained from the raw intensity values using the robust multiarray analysis preprocessing algorithm available in the library AffyPLM using default settings (23). Gene expression changes were calculated as ratios between SCFA infusions and the control group. Metabolic pathways and genes were retrieved from the KEGG database. Array data are available at the Gene Expression Omnibus under accession no. GSE45926.

Statistics. All data are presented as mean values ± SE. Statistical analysis was assessed by one-way ANOVA using the Tukey test for post hoc analysis. Statistical significance was reached at a P value below 0.05.

RESULTS

In vivo cecal infusion of SCFAs in conscious mice. We developed a new method to infuse conscious mice directly in the cecum with stable SCFA isotopes. When the cannula was inserted directly in the cecum, no peristaltic malfunction occurred, in contrast to what was observed when the cannula was inserted in the cecum via the small intestine or colon (unpub-

lished observations). Animals regained presurgery weight after 3 days. Cecal cannulas were flushed daily to prevent obstruction. Infusion rates of 0.2 ml/h did not cause discomfort to the mice, and no back flush in the small intestine or flushing of the colon was observed (observations using carmine). Labeled SCFAs were infused at a concentration of 0.3 M, resulting in a delivery rate of ~2.4 mmol·kg^{-1}·h^{-1}, depending on the exact body weight. This ensured substantial isotope enrichment in the metabolic intermediates after 6 h.

SCFAs are interconverted by gut microbiota. To investigate bacterial SCFA interconversion in the cecum, the enrichments of cecal SCFAs were measured after a 6-h infusion. Approximately 80–100% of SCFA in the cecum was replaced by the infused isotope (Fig. 1*A*). Infusion of [1-^{13}C]acetate resulted in single (M^{+1})- and double (M^{+2})-labeled butyrate, indicating dimerization of either one labeled acetate and one nonlabeled endogenous acetate or two labeled acetate, respectively. Hardly any label from [1-^{13}C]acetate was found in propionate (Fig. 1*A*). Infusion of [2-^{13}C]propionate gave double-labeled butyrate but no single labeled, suggesting that two labeled propionate molecules were used to synthesize one molecule of double-labeled butyrate. The label enrichment in butyrate produced from propionate was approximately threefold lower compared with butyrate synthesized from acetate (23.3 ± 4.7 and 61.8 ± 4.1%, respectively). Hardly any label from [2-^{13}C]propionate was found in acetate (Fig. 1*A*). When [2,4-$^{13}C_2$]butyrate was infused, single-labeled acetate and propionate were found in the cecum (12.3 ± 3.0 and 22.5 ± 4.5%, respectively), showing that gut microbiota convert butyrate into acetate and propionate (Fig. 1*A*). Overall, these results indicate that there is a high interconversion from acetate to butyrate, a low interconversion from butyrate to acetate and between butyrate and propionate, and almost no interconversion between acetate and propionate (Fig. 1*D*).

SCFAs are taken up by the host and transported into the bloodstream. To assess to which extent gut-derived SCFAs are taken up by the host and reach organs beyond the gastrointestinal tract, we measured the isotopic enrichment of SCFAs in the plasma of the mice (Fig. 1*B*). The infused [1-^{13}C]acetate was diluted ninefold in the plasma compared with the cecum

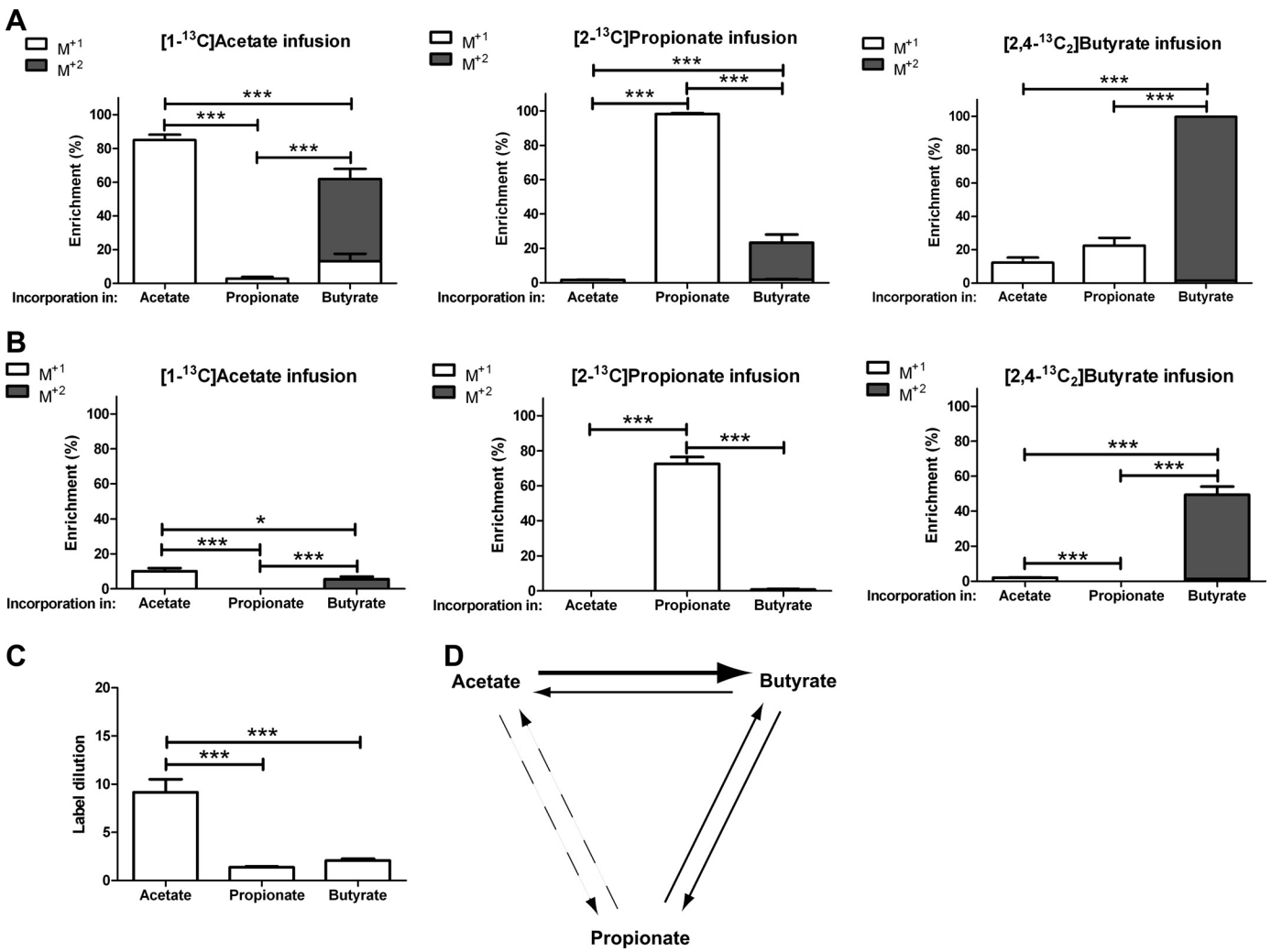

Fig. 1. Single (M^{+1})- and double (M^{+2})-labeled enrichments of acetate, propionate, and butyrate in cecum (*A*) and plasma (*B*) after a 6-h cecal infusion with [1-^{13}C]acetate, [2-^{13}C]propionate, or [2,4-$^{13}C_2$]butyrate. *C*: label dilution of acetate, propionate, and butyrate from cecum to plasma calculated from the corresponding infusion. *D*: schematic overview of the interconversion between acetate, propionate, and butyrate. The amount of conversion is depicted by the thickness of the arrow. Data represent means ± SE for $n = 6–7$ experiments. *$P < 0.05$, **$P < 0.01$, and ***$P < 0.001$.

(9.2 ± 1.2), whereas the infused [2-^{13}C]propionate was only slightly diluted between cecum and blood (1.4 ± 0.1; Fig. 1*C*). The infused [2,4-$^{13}C_2$]butyrate was diluted approximately twofold from cecum to blood (2.1 ± 0.2). The high label dilution for acetate indicates a high endogenous acetate metabolism by the host.

Contribution of SCFAs to glucose. Propionate can be converted into succinate, which can subsequently support gluconeogenesis via oxaloacetate. Acetate and butyrate enter the TCA cycle as acetyl-CoA and are converted to citrate, followed by the conversion to succinate and finally oxaloacetate (Fig. 5*D*). Because two carbon atoms are lost in the conversion of citrate into succinate, no net carbon transfer takes place during label transfer from acetate and butyrate to glucose. The carbon atoms lost, however, come from the oxaloacetate moiety in citrate, and, as a consequence, label can be transferred from acetate and butyrate to oxaloacetate, which ends up in triose phosphate and subsequently in glucose.

To investigate label incorporation into glucose, we measured the enrichment in plasma glucose over time during the infusion period and determined the glucose precursor pool enrichment and the fractional glucose flux to the plasma glucose pool by applying MIDA. The glucose precursor pool enrichment is defined as the label enrichment of the biosynthetic precursor subunits (i.e., triose phosphate) that give rise to newly synthesized glucose. It is derived computationally from the ratio of M^{+1} and M^{+2} glucose, assuming that glucose is a dimer of triose phosphate and that the dimerization can be described by a frequency distribution (50). This assumption allows for the calculation of the fractional glucose flux to the total pool of glucose in the compartment of interest (plasma in this case) that has been synthesized from labeled triose phosphate during the infusion experiment (20, 34, 50). Label from the infused SCFAs appeared in glucose already after 1 h infusion and reached isotopic steady state after 4 h of infusion (Fig. 2*A*). During [1-^{13}C]acetate infusion the steady-state glucose enrichment was 2.0 ± 0.1 and 0.1 ± 0.01% for M^{+1} and M^{+2}, respectively. The [2-^{13}C]propionate infusion resulted in an enrichment of 19 ± 1.1 and 3 ± 0.4% for M^{+1} and M^{+2}, respectively, at steady state. The infusion of [2,4-$^{13}C_2$]butyrate resulted in a higher glucose enrichment compared with acetate, 11 ± 0.7 and 2 ± 0.3% for M^{+1} and M^{+2}, respectively. The calculated enrichment of the triose phosphate precursor pool increased from acetate to propionate to butyrate as substrates (2.8 ± 0.5, 17.6 ± 1.5, and 25.9 ± 0.9%, respectively; Fig. 2*B*). Irrespective of the pronounced differences in enrichment of the triose phosphate precursor pool during acetate and butyrate infusions, the fractional glucose flux to the total plasma pool of glucose was very similar for acetate and butyrate (39.0 ± 5.4 and 34.0 ± 1.4%, respectively), but almost half of what had been observed with propionate as the substrate (69.1 ± 2.4%; Fig. 2*C*).

Incorporation of SCFAs into fatty acids. To assess hepatic synthesis of different fatty acids from SCFAs we determined hepatic enrichment of palmitate (C16:0) and stearate (C18:0) in four different lipid classes: cholesterylesters (CE), free fatty acids (FFA), triglycerides (TG), and phospholipids (PL). All three SCFA infusions resulted in label incorporation into palmitic acid in all four lipid classes. Similar to glucose, MIDA algorithms applied to fatty acids in these lipid classes allows for the calculation of the precursor pool enrichment defined as the enrichment of the biosynthetic precursor subunits for newly

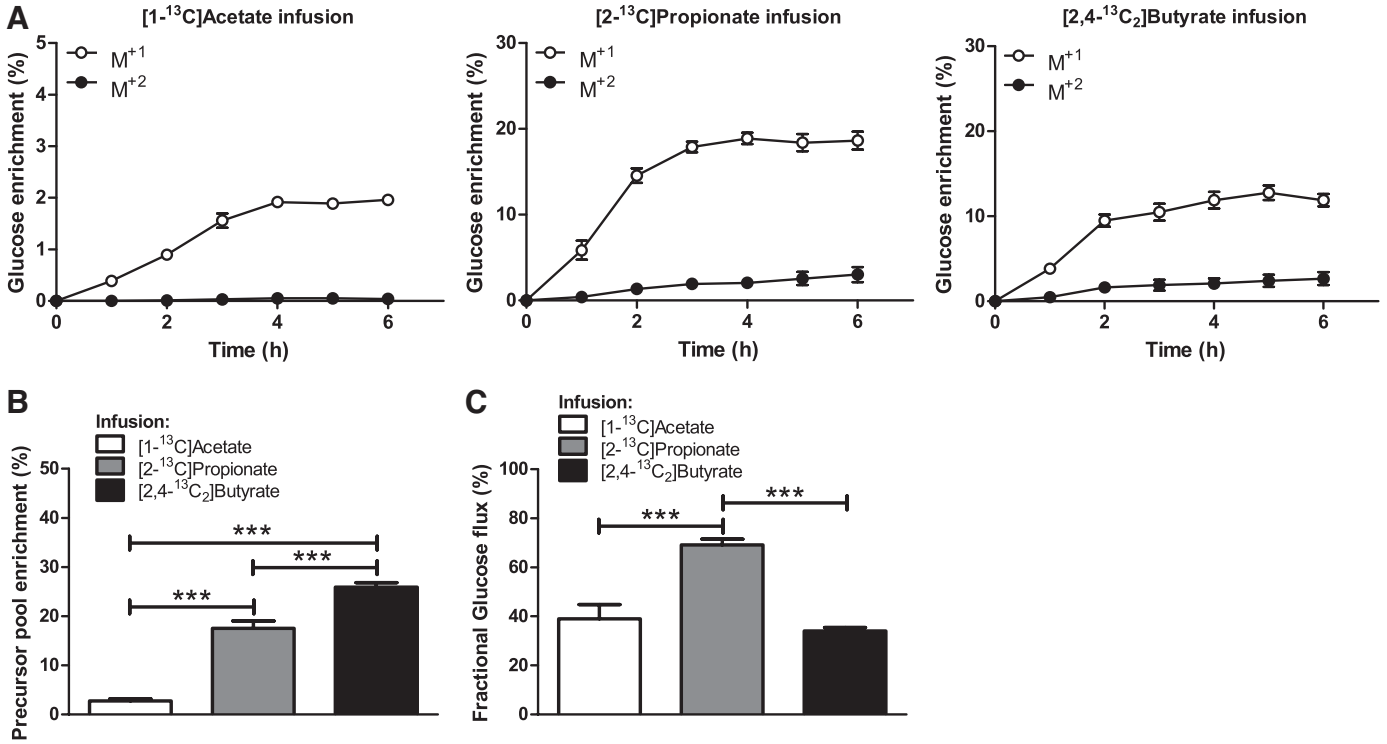

Fig. 2. *A*: M^{+1} and M^{+2} enrichments of plasma glucose during a 6-h cecal infusion with [1-^{13}C]acetate, [2-^{13}C]propionate, or [2,4-$^{13}C_2$]butyrate. Steady-state glucose precursor pool enrichments (*B*) and fractional contribution to glucose flux for acetate, propionate, and butyrate (*C*). Data represent means ± SE for $n = 6$–7. ***$P < 0.001$.

synthesized fatty acids (i.e., acetyl-CoA) and the fractional fatty acid synthesis as the fraction of the pool of fatty acids that was newly synthesized during the infusion experiment (20, 34, 50). The precursor enrichment was calculated from the ratio of M^{+1} and M^{+3} palmitate (34, 35). The acetyl-CoA precursor pool enrichments for palmitate and stearate decreased in the order of butyrate > acetate > propionate as substrates (Fig. 3*A*). FFA and the fatty acyl residues in TG and PL showed comparable precursor enrichments, whereas the precursor enrichment of the fatty acyl residues in CE was approximately two times lower. [1-^{13}C]acetate and [2,4-$^{13}C_2$]butyrate resulted in a similar palmitate fractional synthesis in all lipid classes studied (2.8 ± 0.2 and 2.7 ± 0.4%, respectively), whereas [2-^{13}C]propionate supported a significantly lower lipid fractional synthesis (0.6 ± 0.1%; Fig. 3*B*).

Stearate can either originate from de novo synthesized palmitate or from chain elongation of preexisting palmitate (35). Fractional stearate synthesis from de novo synthesized palmitate was comparable in the four lipid classes (Fig. 3*C*), but lower than the fractional palmitate synthesis (Fig. 3*B*). In addition, no de novo stearate synthesis was observed from [2-^{13}C]propionate. Chain elongation of preexisting palmitate was comparable for acetate and butyrate (7.8 ± 1.0 and 8.6 ± 1.3%, respectively) but not detectable for propionate as substrate (Fig. 3*D*). Fractional synthesis by chain elongation of preexisting palmitate decreased in the order of PL > FFA > TG > CE. In addition, chain elongation was significantly higher than de novo stearate synthesis and palmitate synthesis (Fig. 3, *B–D*).

Acylcarnitines in plasma are used as a proxy of mitochondrial fatty acid oxidation. Changes in the composition of the acylcarnitines in plasma are considered to reflect changes in functioning of the mitochondrial fatty acid oxidation. Accordingly, defects in fatty acid oxidation can be detected by characteristic changes in the acylcarnitine profile. Because the MIDA algorithms applied to the label incorporation into palmitic acid allowed us to calculate the enrichment of the hepatic acetyl-CoA pool, we wondered how these values compared with the enrichment of plasma acetylcarnitine. The measured enrichment of plasma acetylcarnitine was, however, approximately one-third of the average acetyl-CoA precursor enrichment calculated from the label incorporation into the

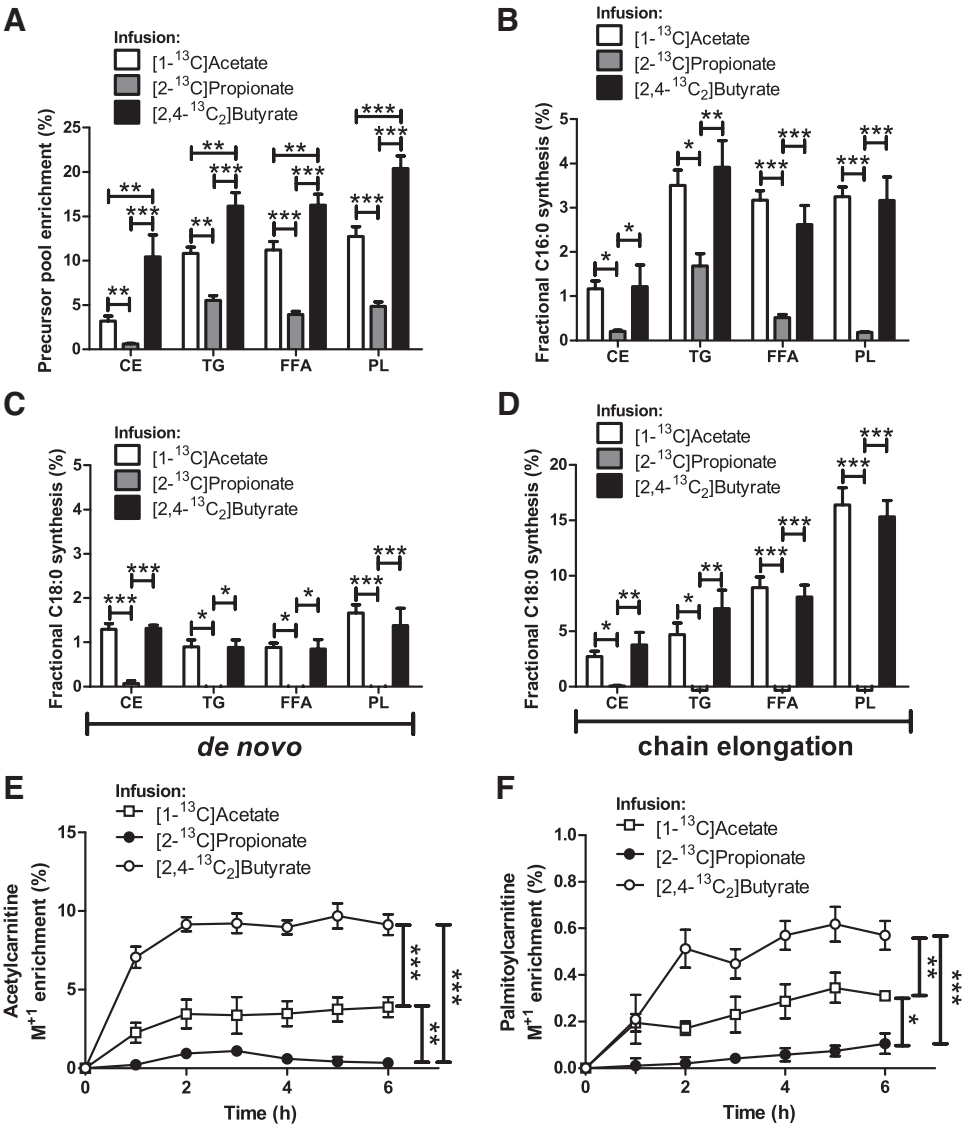

Fig. 3. *A*: hepatic precursor pool enrichments in cholesterylester (CE)-derived, triglyceride (TG)-derived, free fatty acid (FFA)-derived, and phospholipid (PL)-derived palmitate after a 6-h cecal infusion with [1-^{13}C]acetate, [2-^{13}C]propionate, or [2,4-$^{13}C_2$]butyrate. *B*: hepatic fractional synthesis rates of CE-derived, TG-derived, FFA-derived, and PL-derived palmitate (C16:0) from de novo lipogenesis. Fractional stearate (C18:0) synthesis from elongation of de novo synthesized palmitate (*C*) and preexisting palmitate (*D*). M^{+1} enrichment of acetylcarnitine (*E*) and palmitoylcarnitine (*F*) during infusion period. Data represent means ± SE for $n = 6$–7. *$P < 0.05$, **$P < 0.01$, and ***$P < 0.001$.

palmitoyl residue in TG, FFA, and PL lipid fractions (2.1 ± 0.3 and 6.5 ± 1.6%, respectively; Fig. 3, *A* and *E*). It was, however, similar to the precursor enrichment of the CE lipid fraction. Furthermore, the enrichment of acetylcarnitine in plasma showed the same order of decrease as the average of the acetyl-CoA precursor pool enrichments calculated from the label incorporation into the palmitoyl residue in TG, FFA, and PL lipid fractions (butyrate > acetate > propionate). Next, we asked ourselves the question whether newly synthesized palmitate appears in plasma palmitoylcarnitine. As is clear from Fig. 3*F* labeled palmitoylcarnitine did appear in plasma. After 2 h of infusion the steady-state isotope enrichment was reached for the palmitoylcarnitine (Fig. 3*F*). Similar to the label efficiency observed in the palmitate residue in the four lipid classes, label incorporation decreased in the order of butyrate > acetate > propionate. At steady state, enrichment of palmitoylcarnitine was one-third of the average palmitate enrichment in FFA, TG, and PL (0.3 ± 0.1 and 1.0 ± 0.1%, respectively). Apparently, lipogenesis influences the composition of acylcarnitines in plasma as does mitochondrial fatty acid oxidation.

Cholesterol is synthesized from acetate and butyrate but not from propionate. Because cholesterol synthesis also starts from acetyl-CoA we looked into the incorporation of labeled SCFAs into cholesterol. Incorporation of labeled acetate and butyrate into cholesterol was observed after 1 h of infusion and reached isotopic steady state at 4 h of infusion (Fig. 4*A*). At steady state cholesterol enrichment was 0.25 ± 0.03 and 0.08 ± 0.01% for M^{+1} and M^{+3}, respectively, during infusion of [1-^{13}C]acetate. During [2,4-$^{13}C_2$]butyrate infusion steady-state enrichment was 0.28 ± 0.03 and 0.10 ± 0.03% for M^{+1} and M^{+3}, respectively. The infusion with [2-^{13}C]propionate did not result in any significant enrichment of cholesterol, indicating that propionate is not used as a precursor for cholesterol synthesis. The cholesterol precursor pool enrichment was higher for butyrate compared with acetate as substrate (16.1 ± 1.4 and 9.4 ± 0.8%, respectively; Fig. 4*B*). The fractional synthesis for cholesterol was equal for acetate and butyrate as substrates (0.7 ± 0.1 and 0.9 ± 0.2%, respectively) and approximately similar to the fractional palmitate synthesis of CE (1.2 ± 0.2 and 1.2 ± 0.5%, respectively), suggesting that the turnover of fatty acyl residues in the CE pool is determined by the cholesteryl residue exchange with free cholesterol (Figs. 3*B* and 4*C*).

SCFAs are incorporated into plasma intermediates of central carbon metabolism. To determine the role of SCFAs as substrates in whole body energy metabolism we assessed the incorporation of labeled SCFAs into plasma intermediates of central carbon metabolism. Because all organs secrete metabolites into the plasma compartment, the enrichment in plasma metabolites reflects cumulative SCFA metabolism by different organs. For the three-carbon intermediates, pyruvate, lactate, and alanine, enrichment was highest for propionate as a substrate followed by butyrate and acetate (Fig. 5*A*). Also the three consecutive four-carbon intermediates of the TCA cycle, succinate, fumarate, and malate, and the amino acids aspartate and asparagine derived from oxaloacetate showed incorporation of label from SCFAs (Fig. 5, *B* and *D*). The enrichment decreased in the order of butyrate > propionate > acetate as substrates. Surprisingly, enrichment increased from succinate to fumarate and malate, which is opposite to the direction of the oxidative flux through the TCA cycle. Infusion of double-labeled butyrate resulted in single- and double-labeled intermediates. Finally, the enrichments in the five-carbon amino acids glutamate and glutamine, which are produced from α-ketoglutarate,

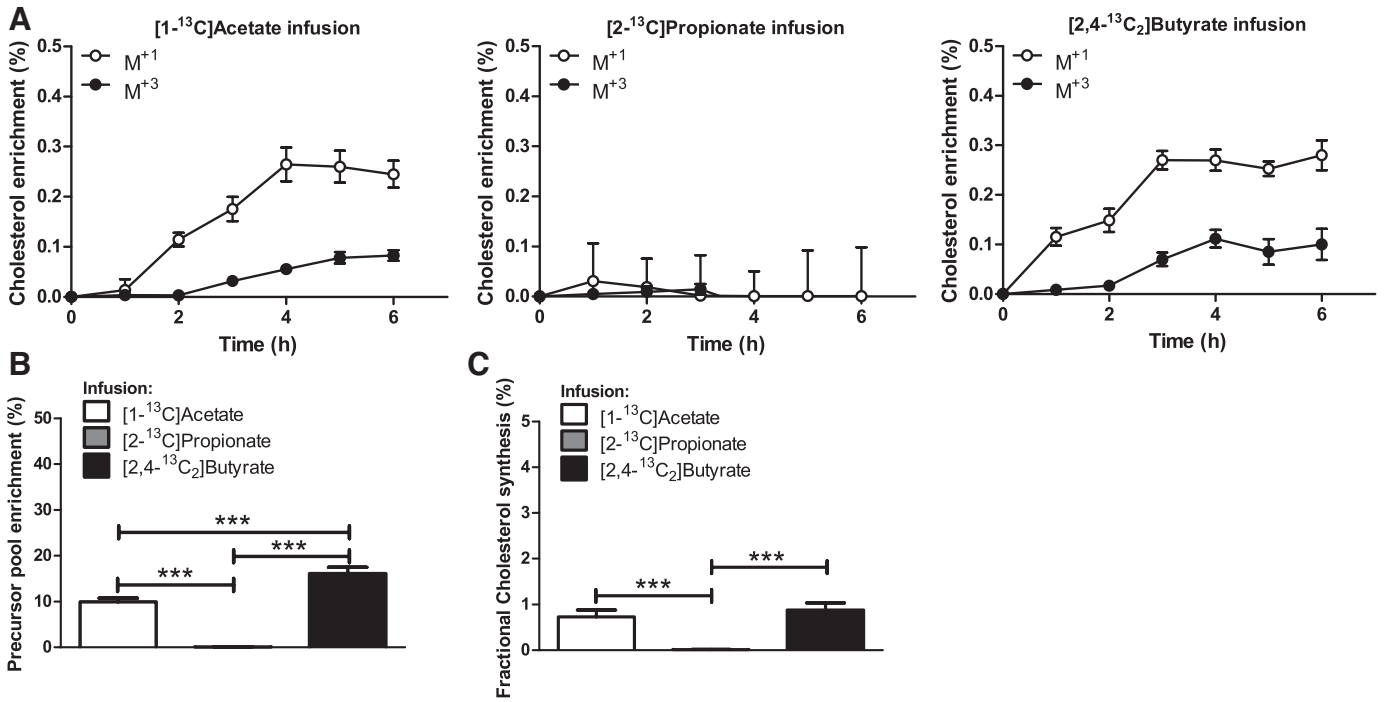

Fig. 4. *A*: M^{+1} and M^{+3} enrichments of plasma cholesterol during a 6-h cecal infusion with [1-^{13}C]acetate, [2-^{13}C]propionate, or [2,4-$^{13}C_2$]butyrate. Steady-state cholesterol precursor pool enrichments (*B*) and fractional synthesis rates of cholesterol for acetate, propionate, and butyrate (*C*). Data represent means ± SE for $n = 6$–7. ***$P < 0.001$.

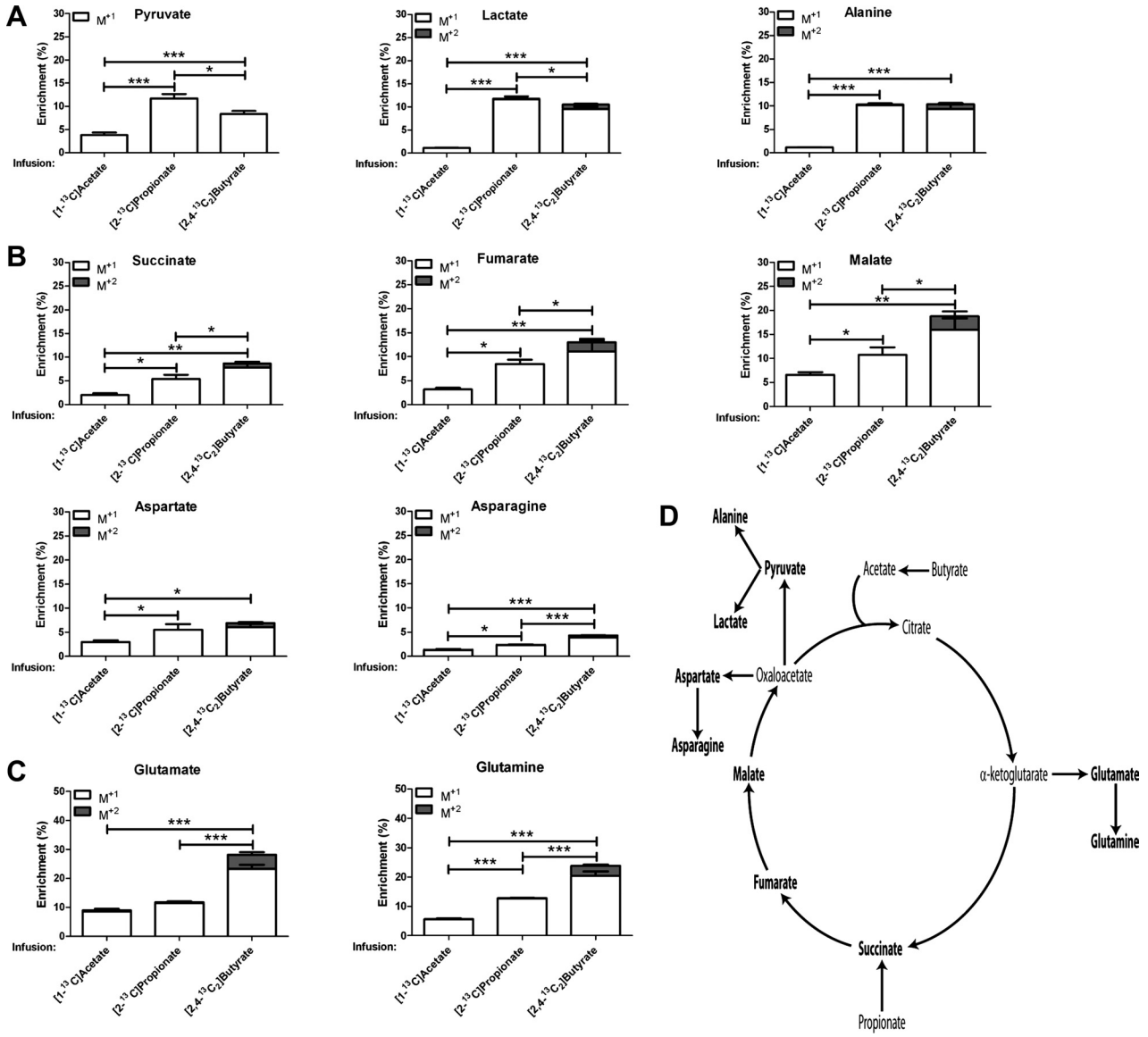

Fig. 5. M^{+1} and M^{+2} enrichments of plasma organic acids and amino acids after a 6-h cecal infusion with [1-^{13}C]acetate, [2-^{13}C]propionate, or [2,4-$^{13}C_2$]butyrate for three-carbon (A), four-carbon (*B*), and five-carbon (*C*) intermediates in central carbon metabolism. *D*: schematic overview of the intermediates in central carbon metabolism with in bold the measured metabolites. Data represent means ± SE for $n = 6$–7. *$P < 0.05$, **$P < 0.01$, and ***$P < 0.001$.

were similar to that of the four-carbon compounds (Fig. 5*C*). Again, the enrichment decreased in the order of butyrate > propionate > acetate as substrates, and butyrate infusion resulted in single- and double-labeled metabolites.

Hepatic SCFA fluxes are mainly regulated at the metabolic level. To assess whether the fluxes of SCFAs into glucose, lipids, cholesterol, and central carbon intermediates induced changes in expression of genes encoding metabolic enzymes, we performed a microarray analysis on liver samples after 6 h of infusion. With some small exceptions, all three SCFAs had only minor effects on the expression of genes encoding enzymes involved in glucose metabolism, fatty acid metabolism, cholesterol metabolism, and central carbon metabolism (Fig. 6). Note that the scale in Fig. 6 only ranges from the ^{2}log ratio of −0.6 to 0.6 corresponding to a 1.5 times down- or upregulation, respectively; and therefore all observed changes are minor. The observed changes did not occur in enzymes known to control these metabolic pathways. In agreement, there was no clear induction or reduction of one of the pathways after SCFA infusion. Although we analyzed pooled samples, a principal component analysis (data not shown) revealed a distinction between all three SCFA infusions. Acetate and propionate infusions, however, were more clustered together than butyrate infusion, underlining the distinct metabolic and regulatory role of the three SCFAs. Altogether, these data indicate that the observed conversion of SCFAs into glucose and lipids after 6 h of infusion was mainly regulated at the metabolic level, i.e., by supply of the substrate rather than by changes in gene expression.

DISCUSSION

This study presents a comprehensive and quantitative in vivo analysis of partitioning of SCFAs over the different metabolic

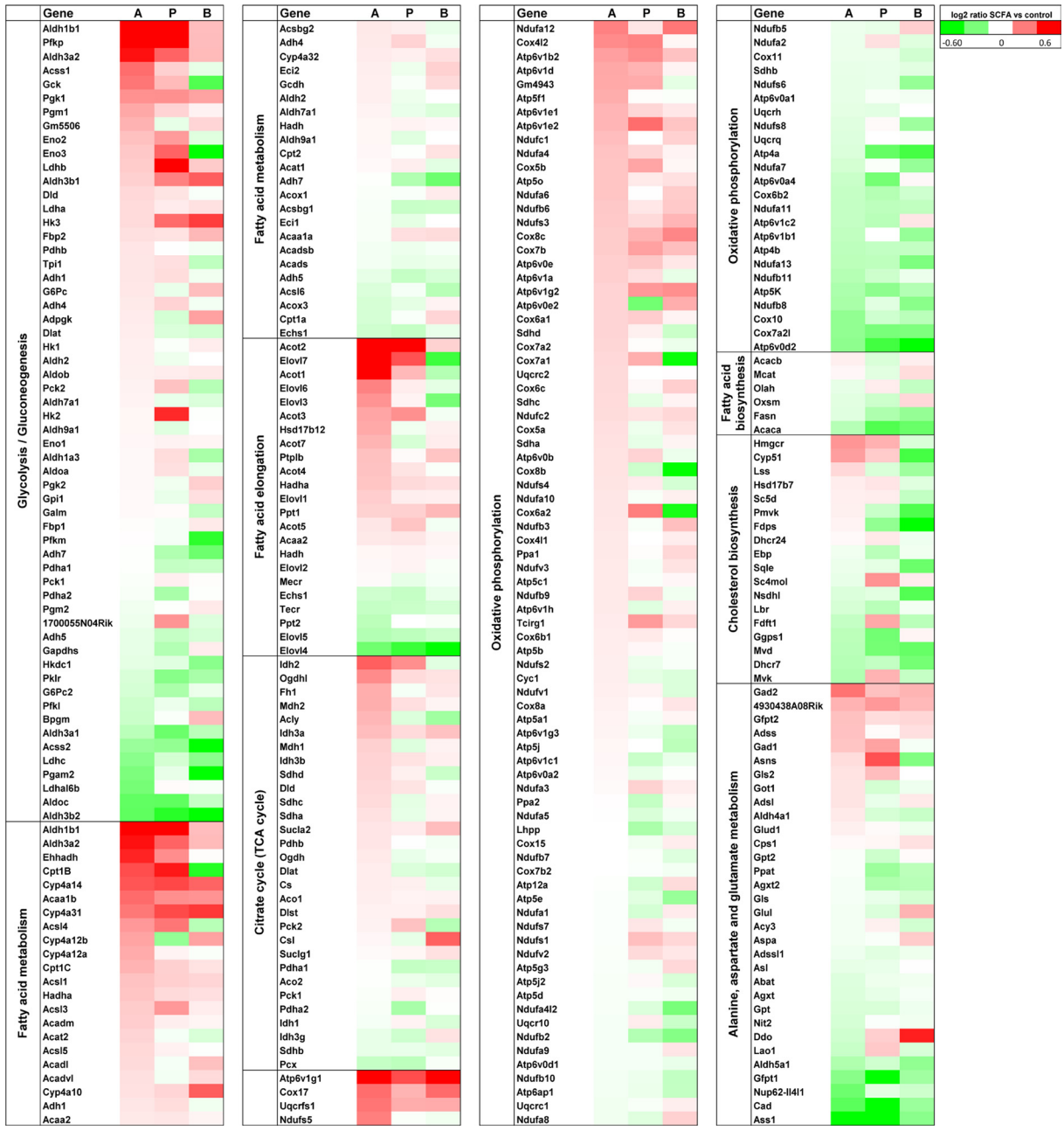

Fig. 6. Heat map of hepatic genes present in the metabolic gene sets derived from the KEGG database after 6 h of infusion with [1-^{13}C]acetate, [2-^{13}C]propionate, or [2,4-$^{13}C_2$]butyrate. Genes are grouped per pathway and can be present in multiple pathways. Data are presented as $^{2}\log([\text{mRNA}]_{\text{SCFA infusion}}/[\text{mRNA}]_{\text{control}})$. The intensity of the red and green color indicates the degree of induction or suppression of a gene, respectively, and ranged from −0.60 (green, downregulation) to 0.60 (red, upregulation). A, acetate; P, propionate; B, butyrate.

routes in the host's carbohydrate and lipid metabolism, starting from their natural site of production. By infusing stable isotope-labeled SCFAs in physiological quantities directly in the cecum, we quantified bacterial interconversion of SCFAs in the cecum and assimilation of SCFAs in host metabolites. The interconversion of SCFAs in the cecum implies extensive cross-feeding among gut microbiota. The SCFAs that are transported from the lumen of the gut into the host are substrates for central carbon, glucose, fatty acid, and cholesterol metabolism. We confirm the hypothesis that there is a distinct host metabolism of propionate on the one hand and acetate and butyrate on the other hand. More surprisingly, acetate and butyrate incorporation into glucose differs from each other, as we discuss below.

In our study we infused equal amounts of all three SCFAs separately in the cecum. Although this allowed us to study the effects of each SCFA individually, we should note that in our model under physiological conditions SCFAs are present in the cecum in a mixture of 33.3 ± 3.2, 4.5 ± 0.4, and 3.6 ± 0.5 mM for acetate, propionate, and butyrate, respectively. However, various nutritional conditions (i.e., dietary fibers with unique physiochemical properties) elicit different SCFA profiles (11). In our study, the infused SCFA species was always dominant, and this is likely to affect the competition between SCFA for

interconversion. Future quantitative studies should take this into account.

This study and others showed cross-feeding between acetate-producing and butyrate-producing bacteria (15, 44). The gut microbiota consists of a large community of different bacteria that is stabilized by such mutual cross-feeding (16). We also observed bacterial interconversion between propionate and butyrate, but not between propionate and acetate. Infusing single-labeled propionate resulted in double-labeled butyrate, indicating that species in the gut microbiome produce butyrate from two molecules of propionate with concomitant loss of two carbon atoms. Tholozan et al. (48) showed that butyrate could be formed from a single molecule of propionate by direct carboxylation, but they found no evidence for a dimerization reaction. From the relative frequencies of single- and double-labeled butyrate during propionate infusion, we calculated the enrichment of the monomeric precursor pool leading to butyrate, based on MIDA algorithms (20). This precursor pool was 96.5 ± 3.9% enriched, hence almost identical to the measured cecal propionate enrichment (98.1 ± 1.1%) during [2-^{13}C]propionate infusion. Because no label appeared in acetate during [2-^{13}C]propionate infusion, we conclude that cecal acetate is not an intermediate in the dimerization of propionate to butyrate. It is possible, though, that intracellular acetyl-CoA is an intermediate without exchanging with extracellular cecal acetate. Analogously, the [1-^{13}C]acetate infusion experiment yielded a monomeric precursor pool enrichment for formation of butyrate of 88.1 ± 4.2%, which compares favorably with the observed acetate enrichment in this experiment (85.0 ± 3%). This confirms the importance of the well-known dimerization of acetate to butyrate (38). The observed cross-feeding is clinically very interesting. Microbial dysbiosis observed in many metabolic diseases can alter SCFA production and cross-feeding rates, leading to changes in colonic SCFA concentrations and ratios. Tributyrin, a butyrate produg, has been shown to reduce mucosal damage and intestinal permeability in experimental colitis (29). In addition, tributyrin has been shown to attenuate obesity-associated inflammation and insulin resistance (52). These results indicate that increasing butyrate concentrations can increase colonic health but also beneficially impact other organs like liver and adipose tissue. Possibly, similar effects can be reached by stimulating interconversion from acetate to butyrate using clinically interesting pre- or probiotics.

It has been calculated that humans rapidly absorb ~95% of the produced SCFAs, and these SCFAs contribute to ~10% of the human caloric requirements (43). The surprisingly high label dilution for acetate indicates a high endogenous acetate metabolism by the host. Indeed, it has been shown that the oxidation of acetate in the liver proceeds at a slower rate than its formation (46); thus, a considerable quantity of unlabeled acetate should be released from the liver. If we explain the label dilution entirely from endogenous production, this implies that the steady-state endogenous acetate production is 22 $mmol \cdot kg^{-1} \cdot h^{-1}$ and that the colonic contribution of acetate is ~10%. Pouteau et al. (37) performed whole body stable-isotope dilution studies by intravenous infusion of labeled acetate in fasted humans before and after giving them 20 g of pure lactulose as a source of acetate production by gut microbiota. From the difference in whole body production between both situations they estimated that colonic acetate production amounted to 35% of total whole body acetate production. The difference with our results can be explained from the different experimental setup, from the different organisms, and from the fact that we take both the enrichment in the cecum and in the plasma into account, which gives a more reliable estimation of the colonic contribution.

Label from all three SCFAs is incorporated in glucose. Propionate is a known gluconeogenic substrate that enters the TCA cycle as succinyl-CoA and is then converted into oxaloacetate. By contrast, label incorporation from acetate and butyrate can be fully explained by the well-known label transfer from [1-^{13}C]acetate and [2,4-$^{13}C_2$]butyrate to oxaloacetate in the TCA cycle (53), a process in which no net glucose synthesis from SCFAs occurs. Theoretically, however, net synthesis from acetate and butyrate to glucose has been proposed via formation of acetone, which is then converted to pyruvate by cytochrome *P*-450 2E1 (Cyp2e1) (24). Experimental studies in humans showed that glucose production from acetone is increasing during prolonged fasting (39). We observed no induction of Cyp2e1 expression or other genes in this pathway by SCFAs (Table 1). In light of this observation and because our mice did not undergo prolonged fasting, we consider it most likely that our results are due to classical label transfer, rather than to the Cyp2e1 pathway.

We analyzed label incorporation into plasma glucose quantitatively by MIDA algorithms. This allowed us to estimate *1*) the extent of label incorporation into the triose phosphate precursor pool and *2*) the fractional contribution of labeled SCFAs to plasma glucose, independent of the precursor pool enrichment. Incorporation of label from butyrate into triose phosphate was higher than incorporation from the other SCFAs. Labeling of triose phosphate by acetate was only 10% of that observed during [^{13}C]butyrate infusion. This raises questions about the metabolic pathway by which label derived from acetate gets incorporated into triose phosphate. In the host, labeled acetate can be converted by acetyl-CoA synthetase into labeled acetyl-CoA in the cytosol. Acetyl-CoA must then be imported into mitochondria to be converted into labeled oxaloacetate in the TCA cycle. In contrast, β-oxidation of butyrate delivers acetyl-CoA to the TCA cycle, all of which takes place in mitochondria.

Next, we evaluated the fractional contribution of labeled SCFAs to the plasma glucose flux. Only for propionate this

Table 1. *Hepatic mRNA expression in the acetone pathway from fatty acids to glucose via Cyp2e1*

Gene	Control Infusion	[1-^{13}C]Acetate Infusion	[2-^{13}C]Propionate Infusion	[2,4-$^{13}C_2$]Butyrate Infusion
Cyp2e1	1.0 ± 0.1	1.1 ± 0.1	0.8 ± 0.1	1.0 ± 0.1
Slc16a1	1.0 ± 0.2	1.2 ± 0.1	1.3 ± 0.1	1.2 ± 0.1
PC	1.0 ± 0.1	1.0 ± 0.2	0.8 ± 0.2	0.8 ± 0.2

Values are means ± SE. Cyp2e1, cytochrome *P*-450 2E1; Slc16a1, solute carrier family 16, member 1; PC, pyruvate carboxylase.

represents net glucose synthesis (see below), but for acetate and butyrate it reflects label exchange in the TCA cycle. Irrespective of the difference in labeling efficiencies of triose phosphate, infusion of propionate resulted in the highest fractional glucose flux (69.1 ± 2.4%), whereas infusion of acetate and butyrate resulted in a lower contribution (39.0 ± 5.4 and 34.0 ± 1.4%, respectively). Interpretation of this observation remains as yet speculative. Differences in labeling efficiency of the triose phosphate pool could not account for it, since the MIDA algorithm corrects for them. If the glucose in all three SCFA infusions is produced via the same triose phosphate pool and if our infusions can be considered to be tracer amounts, then the fractional glucose flux should be the same in all three SCFA infusions. Indeed we infused more than tracer amounts, which may explain part of the discrepancy (see below). Additionally, there might exist a source of plasma glucose that is synthesized from another triose phosphate pool that is inaccessible to labeling. The relative contribution of this unlabeled source is smallest in the case of propionate infusion and larger in the case of butyrate or acetate infusion. The contribution of different organs to whole body gluconeogenesis varies, with liver being the most important, followed by the kidneys, and gut being the smallest contributor (32). Therefore, differences in the ability to metabolize individual SCFAs by gut, liver, and kidneys might have caused the observed difference between the three SCFAs in fractional contribution of labeled glucose to plasma glucose. Finally, because we infused labeled SCFAs at high physiological rates, an increased whole body gluconeogenic flux from the infused propionate would be expected, which might also account for the high fractional glucose flux of 69.1%. Conversely, also a very high proportion of the label in infused butyrate is incorporated into glucose. To achieve the glucose production normally observed in C57Bl/6J mice in our laboratory [100 $\mu mol \cdot kg^{-1} \cdot min^{-1}$ (12)], it would require 62% of propionate infused. If the glucose production is increased due to the infusion, this percentage would even be higher. Altogether, we conclude that the gut-derived propionate is largely used for glucose production and that this process has a high flexibility toward increased propionate production.

Palmitate and cholesterol were mostly synthesized from acetate and butyrate. The contribution of propionate to palmitate synthesis was small but detectable, as previously reported (40). Propionate did not contribute to cholesterol synthesis. Also stearate was only labeled by acetate and butyrate, and not by propionate. In agreement with earlier observations label from SCFAs entered stearate via chain elongation of preexisting palmitate and not so much via de novo synthesis (34, 35). The approximately twofold higher rate of chain elongation in stearate from PL compared with TG and FFA was also observed by Zambell et al. (54). The fact that we found label incorporation into plasma acetylcarnitine and palmitoylcarnitine shows that the plasma acylcarnitine pool is not only a reflection of fatty acid β-oxidation as stated by others (1, 25) but also of fatty acid synthesis.

Next to incorporation of SCFAs by the liver in glucose and fatty acids, we also measured enrichments in intermediates of central carbon metabolism in plasma as a reflection of whole body SCFA metabolism. Surprisingly, for all three SCFAs the enrichment increased in the direction of the flux through the TCA cycle, from succinate to fumarate and malate. Because acetate and butyrate enter the TCA cycle as acetyl-CoA and propionate as succinyl-CoA, we would expect that the enrichment would decrease from succinate to malate. The lower enrichments in succinate and fumarate indicates an influx of unlabeled metabolites into the plasma compartment from other (not labeled) organs.

Next to the role of SCFAs as substrates, we also assessed whether they might induce gene expression by performing a microarray analysis on liver after 6 h infusion. The small changes in expression of genes involved in metabolic pathways indicate that SCFAs play only a minor role in the regulation of the hepatic gene expression at this time scale. Hence, the observed SCFA metabolism can be attributed largely to preexisting enzymes.

In conclusion, we developed a mouse model in which we infused SCFAs directly in the cecum and showed that there is considerable microbial interconversion between acetate and butyrate as well as between propionate and butyrate. Cecal acetate and butyrate are important substrates for mammalian lipid metabolism, whereas propionate strongly contributes to gluconeogenesis. Furthermore, mitochondrial metabolism of acetate appears to be minimal, in contrast to butyrate. These aspects are key if we aim to understand their strong effects on mammalian carbon and energy metabolism, next to their known role as ligands and regulators.

GRANTS

This work was funded by the Netherlands Genomics Initiative via the Netherlands Consortium for Systems Biology.

DISCLOSURES

The authors declare no conflicts of interest, financial or otherwise, associated with this work.

AUTHOR CONTRIBUTIONS

Author contributions: G.d.B., B.M.B., and D.-J.R. conception and design of research; G.d.B. and R.H. performed experiments; G.d.B., K.L., T.H.v.D., and A.G. analyzed data; G.d.B., K.L., T.H.v.D., K.v.E., M.M., A.K.G., G.J.E.J.H., B.M.B., and D.-J.R. interpreted results of experiments; G.d.B. prepared figures; G.d.B., B.M.B., and D.-J.R. drafted manuscript; G.d.B., K.L., K.v.E., A.K.G., G.J.E.J.H., B.M.B., and D.-J.R. edited and revised manuscript; G.d.B., K.L., R.H., T.H.v.D., A.G., K.v.E., M.M., A.K.G., G.J.E.J.H., B.M.B., and D.-J.R. approved final version of manuscript.

REFERENCES

1. **Adams SH, Hoppel CL, Lok KH, Zhao L, Wong SW, Minkler PE, Hwang DH, Newman JW, Garvey WT.** Plasma acylcarnitine profiles suggest incomplete long-chain fatty acid β-oxidation and altered tricarboxylic acid cycle activity in type 2 diabetic African-American women. *J Nutr* 139: 1073–1081, 2009.
2. **Anderson JW, Bridges SR.** Short-chain fatty acid fermentation products of plant fiber affect glucose metabolism of isolated rat hepatocytes. *Proc Soc Exp Biol Med* 177: 372–376, 1984.
3. **Bergman EN.** Energy contributions of volatile fatty acids from the gastrointestinal tract in various species. *Physiol Rev* 70: 567–590, 1990.
4. **Binder HJ.** Role of colonic short-chain fatty acid transport in diarrhea. *Annu Rev Physiol* 72: 297–313, 2010.
5. **Bloemen JG, Venema K, van de Poll MC, Olde Damink SW, Buurman WA, Dejong CH.** Short chain fatty acids exchange across the gut and liver in humans measured at surgery. *Clin Nutr* 28: 657–661, 2009.
6. **Breuer RI, Buto SK, Christ ML, Bean J, Vernia P, Paoluzi P, Di Paolo MC, Caprilli R.** Rectal irrigation with short-chain fatty acids for distal ulcerative colitis. Preliminary report. *Dig Dis Sci* 36: 185–187, 1991.
7. **Clausen MR, Mortensen PB.** Kinetic studies on the metabolism of short-chain fatty acids and glucose by isolated rat colonocytes. *Gastroenterology* 106: 423–432, 1994.
8. **Dai M, Wang P, Boyd AD, Kostov G, Athey B, Jones EG, Bunney WE, Myers RM, Speed TP, Akil H, Watson SJ, Meng F.** Evolving gene/transcript definitions significantly alter the interpretation of GeneChip data (Abstract). *Nucleic Acids Res* 33: e175, 2005.

9. **de Wit N, Bosch-Vermeulen H, de Groot P, Hooiveld GJ, Bromhaar M, Jansen J, Muller M, van der Meer R.** The role of the small intestine in the development of dietary fat-induced obesity and insulin resistance in C57BL/6J mice. *BMC Medical Genomics* 1: 14–30, 2008.
10. **Demigné C, Morand C, Levrat MA, Besson C, Moundras C, Rémésy C.** Effect of propionate on fatty acid and cholesterol synthesis and on acetate metabolism in isolated rat hepatocytes. *Br J Nutr* 74: 209–219, 1995.
11. **den Besten G, van Eunen K, Groen AK, Venema K, Reijngoud D, Bakker BM.** The role of short-chain fatty acids in the interplay between diet, gut microbiota and host energy metabolism. *J Lipid Res* 54: 2325–2340, 2013.
12. **Derks TG, van Dijk TH, Grefhorst A, Rake JP, Smit GP, Kuipers F, Reijngoud DJ.** Inhibition of mitochondrial fatty acid oxidation in vivo only slightly suppresses gluconeogenesis but enhances clearance of glucose in mice. *Hepatology* 47: 1032–1042, 2008.
13. **Di Sabatino A, Morera R, Ciccocioppo R, Cazzola P, Gotti S, Tinozzi FP, Tinozzi S, Corazza GR.** Oral butyrate for mildly to moderately active Crohn's disease. *Aliment Pharmacol Ther* 22: 789–794, 2005.
14. **Donohoe DR, Garge N, Zhang X, Sun W, O'Connell TM, Bunger MK, Bultman SJ.** The microbiome and butyrate regulate energy metabolism and autophagy in the mammalian colon. *Cell Metab* 13: 517–526, 2011.
15. **Duncan SH, Holtrop G, Lobley GE, Calder AG, Stewart CS, Flint HJ.** Contribution of acetate to butyrate formation by human faecal bacteria. *Br J Nutr* 91: 915–923, 2004.
16. **Flint HJ, Duncan SH, Scott KP, Louis P.** Interactions and competition within the microbial community of the human colon: links between diet and health. *Environ Microbiol* 9: 1101–1111, 2007.
17. **Gao Z, Yin J, Zhang J, Ward RE, Martin RJ, Lefevre M, Cefalu WT, Ye J.** Butyrate Improves Insulin Sensitivity and Increases Energy Expenditure in Mice. *Diabetes* 58: 1509–1517, 2009.
18. **Harig JM, Soergel KH, Komorowski RA, Wood CM.** Treatment of diversion colitis with short-chain-fatty acid irrigation. *N Engl J Med* 320: 23–28, 1989.
19. **Havel PJ.** Update on adipocyte hormones: regulation of energy balance and carbohydrate/lipid metabolism. *Diabetes* 53, *Suppl* 1: S143–S151, 2004.
20. **Hellerstein MK, Neese RA.** Mass isotopomer distribution analysis: a technique for measuring biosynthesis and turnover of polymers. *Am J Physiol Endocrinol Metab* 263: E988–E1001, 1992.
21. **Horino M, Machlin LJ, Hertelendy F, Kipnis DM.** Effect of short-chain fatty acids on plasma insulin in ruminant and nonruminant species. *Endocrinology* 83: 118–128, 1968.
22. **Hušek P.** Rapid derivatization and gas chromatographic determination of amino acids. *J Chromatogr A* 552: 289–299, 1991.
23. **Irizarry RA, Hobbs B, Collin F, Beazer-Barclay YD, Antonellis KJ, Scherf U, Speed TP.** Exploration, normalization, and summaries of high density oligonucleotide array probe level data. *Biostatistics* 4: 249–264, 2003.
24. **Kaleta C, de Figueiredo LF, Werner S, Guthke R, Ristow M, Schuster S.** In silico evidence for gluconeogenesis from fatty acids in humans. *PLoS Comput Biol* 7: e1002116, 2011.
25. **Koves TR, Ussher JR, Noland RC, Slentz D, Mosedale M, Ilkayeva O, Bain J, Stevens R, Dyck JRB, Newgard CB, Lopaschuk GD, Muoio DM.** Mitochondrial overload and incomplete fatty acid oxidation contribute to skeletal muscle insulin resistance. *Cell Metab* 7: 45–56, 2008.
26. **Kuliczkowska-Plaksej J, Milewicz A, Jakubowska J.** Neuroendocrine control of metabolism. *Gynecol Endocrinol* 28, *Suppl* 1: 27–32, 2012.
27. **Laurent C, Simoneau C, Marks L, Braschi S, Champ M, Charbonnel B, Krempf M.** Effect of acetate and propionate on fasting hepatic glucose production in humans. *Eur J Clin Nutr* 49: 484–491, 1995.
28. **Lee WN, Byerley LO, Bergner EA, Edmond J.** Mass isotopomer analysis: theoretical and practical considerations. *Biol Mass Spectrom* 20: 451–458, 1991.
29. **Leonel AJ, Teixeira LG, Oliveira RP, Santiago AF, Batista NV, Ferreira TR, Santos RC, Cardoso VN, Cara DC, Faria AM, Alvarez-Leite J.** Antioxidative and immunomodulatory effects of tributyrin supplementation on experimental colitis. *Br J Nutr* 109: 1396–1407, 2013.
30. **Lin K, Kools H, de Groot PJ, Gavai AK, Basnet RK, Cheng F, Wu J, Wang X, Lommen A, Hooiveld GJ, Bonnema G, Visser RG, Muller MR, Leunissen JA.** MADMAX: management and analysis database for multiple ~omics experiments (Abstract). *J Integr Bioinform* 8: 160, 2011.
31. **Moreau NM, Goupry SM, Antignac JP, Monteau FJ, Le Bizec BJ, Champ MM, Martin LJ, Dumon HJ.** Simultaneous measurement of plasma concentrations and 13C-enrichment of short-chain fatty acids, lactic acid and ketone bodies by gas chromatography coupled to mass spectrometry. *J Chromatogr B Analyt Technol Biomed Life Sci* 784: 395–403, 2003.
32. **Mutel E, Gautier-Stein A, Abdul-Wahed A, Amigó-Correig M, Zitoun C, Stefanutti A, Houberdon I, Tourette J, Mithieux G, Rajas F.** Control of blood glucose in the absence of hepatic glucose production during prolonged fasting in mice: induction of renal and intestinal gluconeogenesis by glucagon. *Diabetes* 60: 3121–3131, 2011.
33. **Nishina PM, Freedland RA.** Effects of propionate on lipid biosynthesis in isolated rat hepatocytes. *J Nutr* 120: 668–673, 1990.
34. **Oosterveer MH, Grefhorst A, van Dijk TH, Havinga R, Staels B, Kuipers F, Groen AK, Reijngoud DJ.** Fenofibrate simultaneously induces hepatic fatty acid oxidation, synthesis, and elongation in mice. *J Biol Chem* 284: 34036–34044, 2009.
35. **Oosterveer MH, van Dijk TH, Tietge UJ, Boer T, Havinga R, Stellaard F, Groen AK, Kuipers F, Reijngoud DJ.** High fat feeding induces hepatic fatty acid elongation in mice. *PLoS One* 4: 6: e6066, 2009.
36. **Pouteau E, Nguyen P, Ballevre O, Krempf M.** Production rates and metabolism of short-chain fatty acids in the colon and whole body using stable isotopes. *Proc Nutr Soc* 62: 87–93, 2003.
37. **Pouteau E, Vahedi K, Messing B, Flourie B, Nguyen P, Darmaun D, Krempf M.** Production rate of acetate during colonic fermentation of lactulose: a stable-isotope study in humans. *Am J Clin Nutr* 68: 1276–1283, 1998.
38. **Pryde SE, Duncan SH, Hold GL, Stewart CS, Flint HJ.** The microbiology of butyrate formation in the human colon. *FEMS Microbiol Lett* 217: 133–139, 2002.
39. **Reichard GA, Haff AC, Skutches CL, Paul P, Holroyde CP, Owen OE.** Plasma acetone metabolism in fasting humans. *J Clin Invest* 63: 619–626, 1979.
40. **Reshef L, Niv J, Shapiro B.** Effect of propionate on lipogenesis in adipose tissue. *J Lipid Res* 8: 682–687, 1967.
41. **Roediger WE.** Utilization of nutrients by isolated epithelial cells of the rat colon. *Gastroenterology* 83: 424–429, 1982.
42. **Roy CC, Kien CL, Bouthillier L, Levy E.** Short-chain fatty acids: ready for prime time? *Nutr Clin Pract* 21: 351–366, 2006.
43. **Ruppin H, Bar-Meir S, Soergel KH, Wood CM, Schmitt MGJ.** Absorption of short-chain fatty acids by the colon. *Gastroenterology* 78: 1500–1507, 1980.
44. **Samuel BS, Gordon JI.** A humanized gnotobiotic mouse model of host-archaeal-bacterial mutualism. *Proc Natl Acad Sci USA* 103: 10011–10016, 2006.
45. **Scharlau D, Borowicki A, Habermann N, Hofmann T, Klenow S, Miene C, Munjal U, Stein K, Glei M.** Mechanisms of primary cancer prevention by butyrate and other products formed during gut flora-mediated fermentation of dietary fibre. *Mutat Res* 682: 39–53, 2009.
46. **Skutches CL, Holroyde CP, Myers RN, Paul P, Reichard GA.** Plasma acetate turnover and oxidation. *J Clin Invest* 64: 708–713, 1979.
47. **Tang Y, Chen Y, Jiang H, Robbins GT, Nie D.** G-protein-coupled receptor for short-chain fatty acids suppresses colon cancer. *Int J Cancer* 128: 847–856, 2010.
48. **Tholozan JL, Samain E, Grivet JP, Moletta R, Dubourguier HC, Albagnac G.** Reductive carboxylation of propionate to butyrate in methanogenic ecosystems. *Appl Environ Microbiol* 54: 441–445, 1988.
49. **van der Veen JN, Havinga R, Bloks VW, Groen AK, Kuipers F.** Cholesterol feeding strongly reduces hepatic VLDL-triglyceride production in mice lacking the liver X receptor α. *J Lipid Res* 48: 337–347, 2007.
50. **van Dijk TH, Boer TS, Havinga R, Stellaard F, Kuipers F, Reijngoud DJ.** Quantification of hepatic carbohydrate metabolism in conscious mice using serial blood and urine spots. *Anal Biochem* 322: 1–13, 2003.
51. **Vernia P, Marcheggiano A, Caprilli R, Frieri G, Corrao G, Valpiani D, Di Paolo MC, Paoluzi P, Torsoli A.** Short-chain fatty acid topical treatment in distal ulcerative colitis. *Aliment Pharmacol Ther* 9: 309–313, 1995.
52. **Vinolo MA, Rodrigues HG, Festuccia WT, Crisma AR, Alves VS, Martins AR, Amaral CL, Fiamoncini J, Hirabara SM, Sato FT, Fock RA, Malheiros G, dos Santos MF, Curi R.** Tributyrin attenuates obesity-associated inflammation and insulin resistance in high-fat-fed mice. *Am J Physiol Endocrinol Metab* 303: E272–E282, 2012.
53. **Weinman EO, Strisower EH, Chaikoff IL.** Conversion of fatty acids to carbohydrate: application of isotopes to this problem and role of the krebs cycle as a synthetic pathway. *Physiol Rev* 37: 252–272, 1957.
54. **Zambell KL, Fitch MD, Fleming SE.** Acetate and butyrate are the major substrates for de novo lipogenesis in rat colonic epithelial cells. *J Nutr* 133: 3509–3515, 2003.